Supporting information for

Robust bamboo cellulose/phytic acid composite aerogels with thermal insulation, fire protection and acoustic absorption via ambient pressure drying

Yunyan Zhu[a,b], Sikui Chen[a,b], Yingyang Luo[a,b], Erhui Ren[a,b,d], Hong Tang[e], Ronghui Guo[a,b,c*]

a. College of Biomass Science and Engineering, Sichuan University, Chengdu 610065, China

b. Ministry Education Key Lab Leather Chemistry & Engineering, Sichuan University, Chengdu 610065, Sichuan, China

c. Yibin Industrial Technology Research Institute of Sichuan University, Yibin, Sichuan, China

d. High-Tech Organic Fibers Key Laboratory of Sichuan Province, Chengdu, Sichuan, China

e. Materials Science and Engineering, College of Design and Engineering, National University of Singapore Blk EA, #03-09 9 Engineering Drive 1 Singapore 117575

Content

1. Supporting Figures

2. Supporting Tables

3. References

1. Supporting Figures

*Corresponding Author. Ronghui Guo, E-mail address: ronghuiguo214@126.com

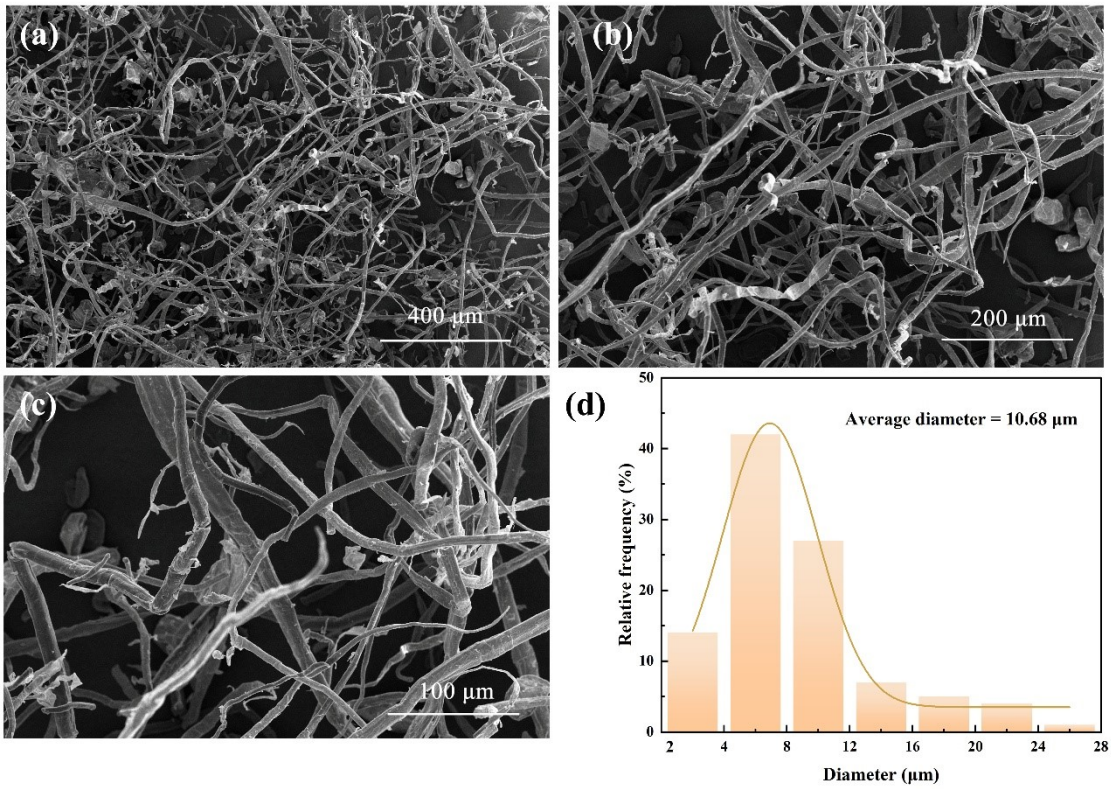

Fig. S1 SEM images (a, b and c) and diameter distribution (d) of bamboo cellulose fibers.

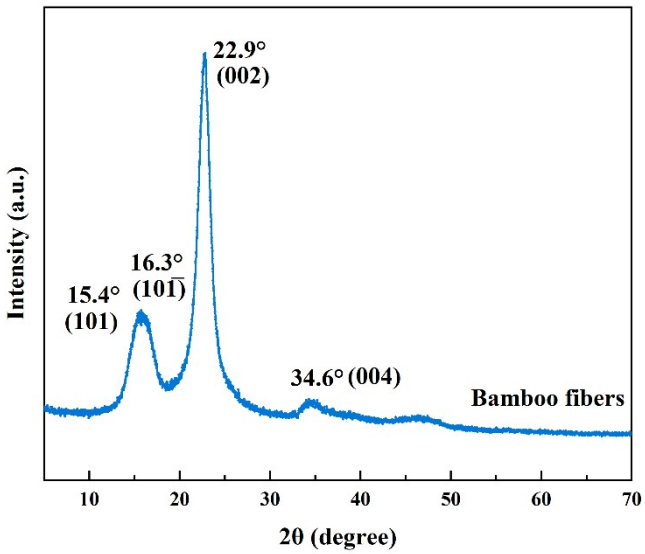

Fig. S2 XRD curve of bamboo cellulose fibers.

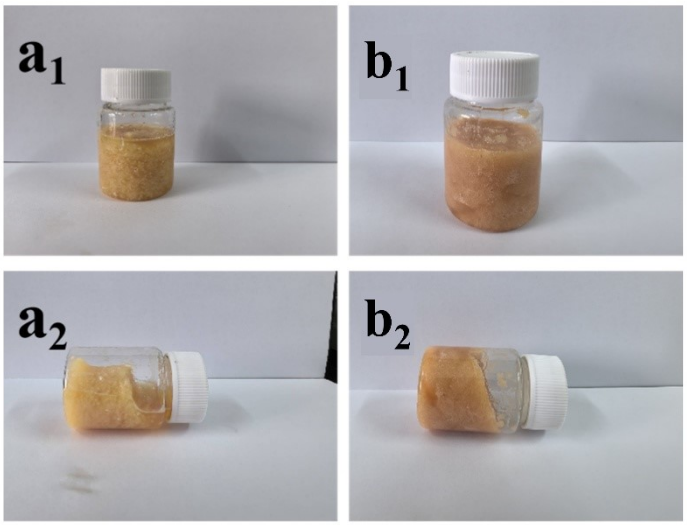

Fig. S3 Digital photos of reaction slurry without CMC (a_1, a_2) and with CMC (b_1, b_2) before freeze molding.

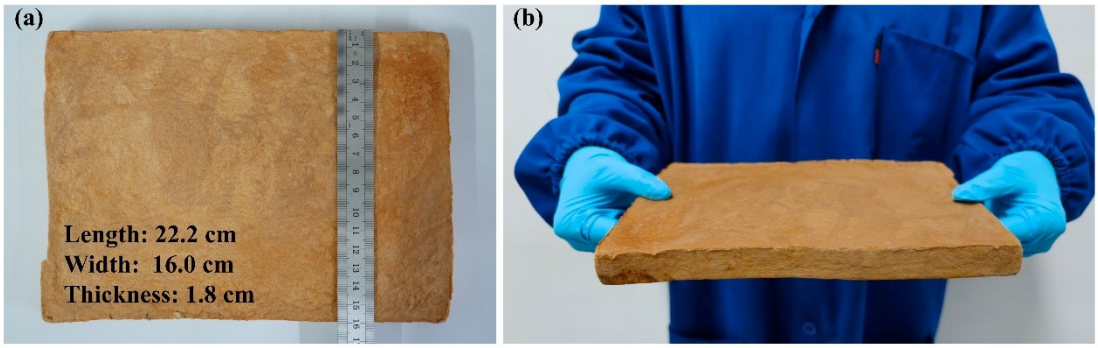

Fig. S4 Digital photos of BCPA aerogel with 15 wt% CMC content and 100 wt% PA content.

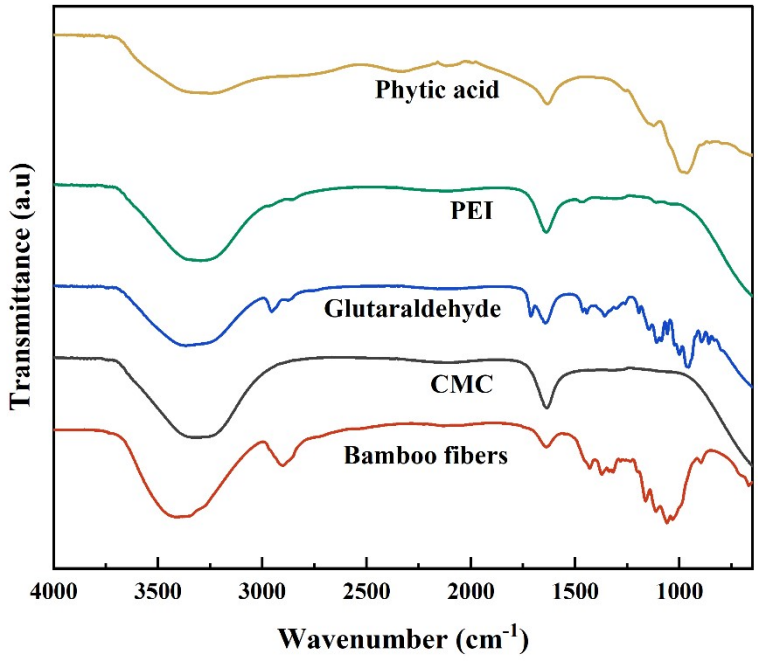
Phytic acid
PEI
Glutaraldehyde
CMC
Bamboo fibers
Transmittance (a.u)
4000
3500
3000
2500
2000
1500
1000
Wavenumber (cm-1)

Fig. S5 FTIR spectra of raw materials in the preparation of BCPA aerogels.

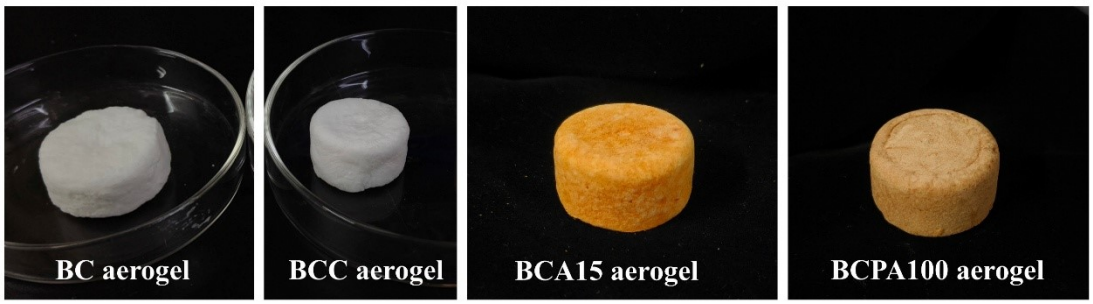

Fig. S6 Digital photos of BC aerogel, BCC aerogel, BCA15 aerogel and BCPA100 aerogel.

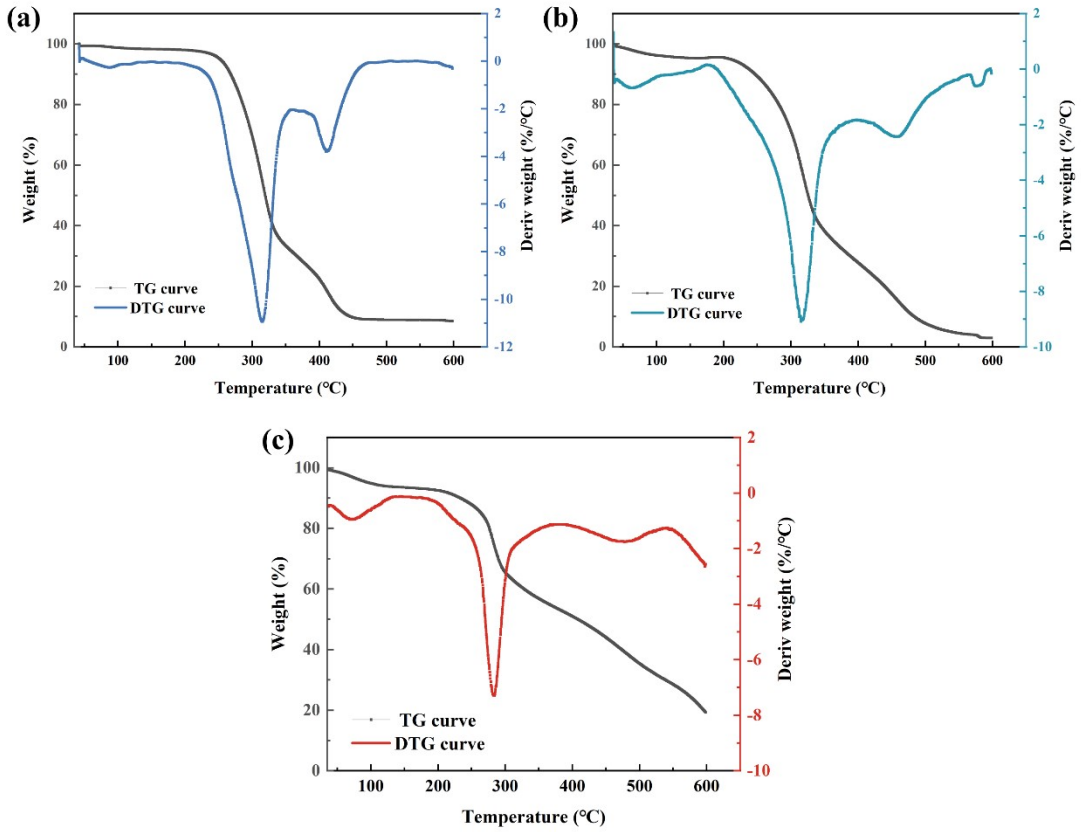

Fig. S7 TG curves and DTG curves of BCC aerogel (BC/GA/CMC), BCA15 aerogel (BC/GA/CMC/PEI) and BCPA100 (BC/GA/CMC/PEI/PA) aerogel under an oxygen atmosphere.

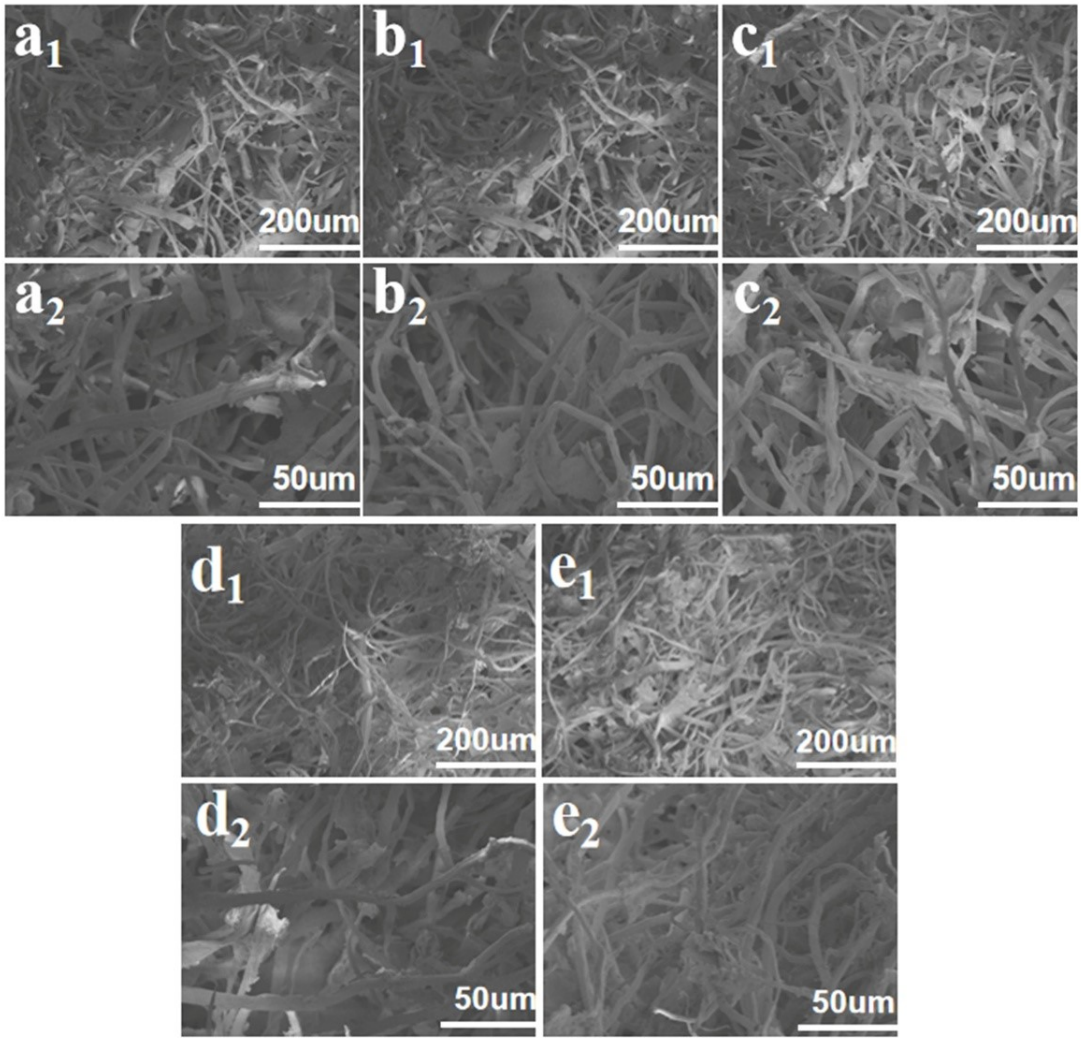

Fig. S8 SEM images of BCA aerogels with different CMC content. (a and a_1) 5 wt%, (b and b_1) 10 wt%, (c and c_1) 15 wt%, (d and d_1) 20 wt% and (e and e_1) 25 wt% at different magnifications.

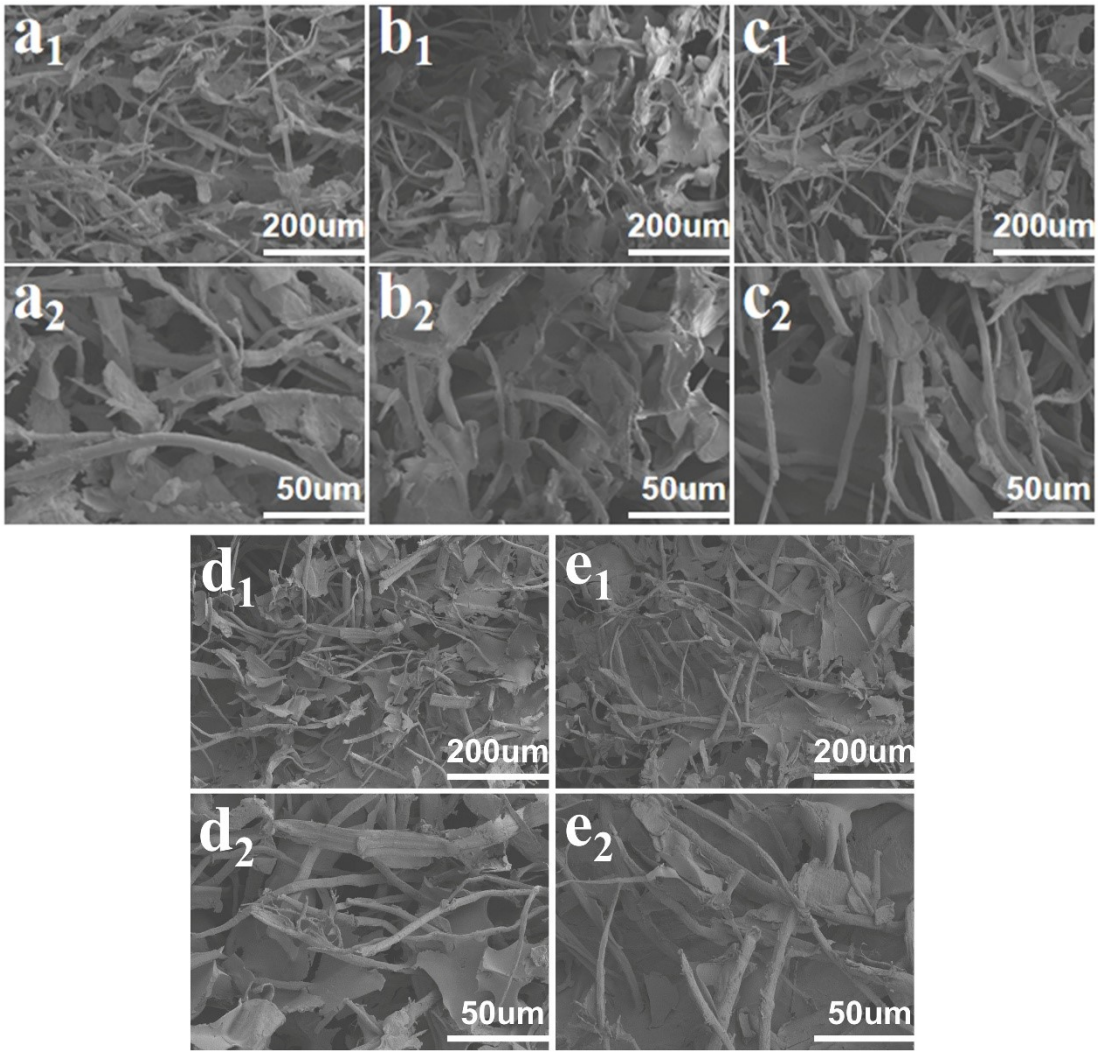

Fig. S9 SEM images of BCPA aerogels with different PA content. (a and a_1) 25 wt%, (b and b_1) 50 wt%, (c and c_1) 75 wt%, (d and d_1) 100 wt% and (e and e_1) 125 wt% at different magnifications.

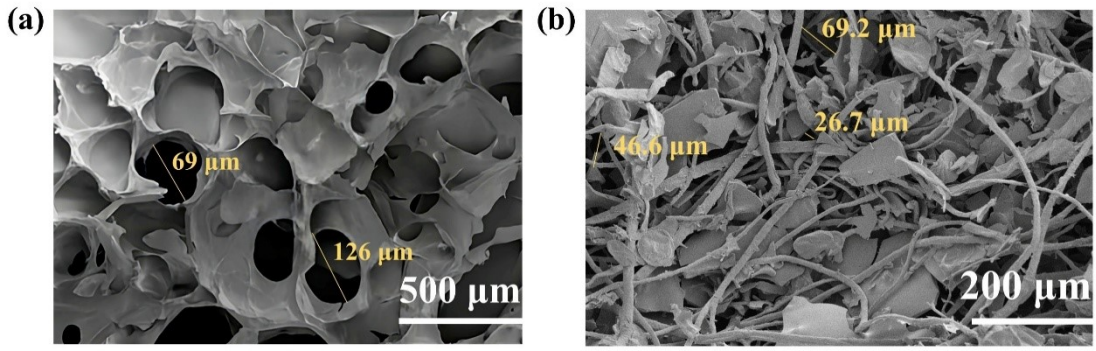

Fig. S10 (a) SEM images of conventional cellulose aerogel prepared via the dissolution–regeneration route (alkali/urea system followed by sol–gel processing and freeze-drying). (b) SEM images of freeze-dried BCPA100 aerogel.

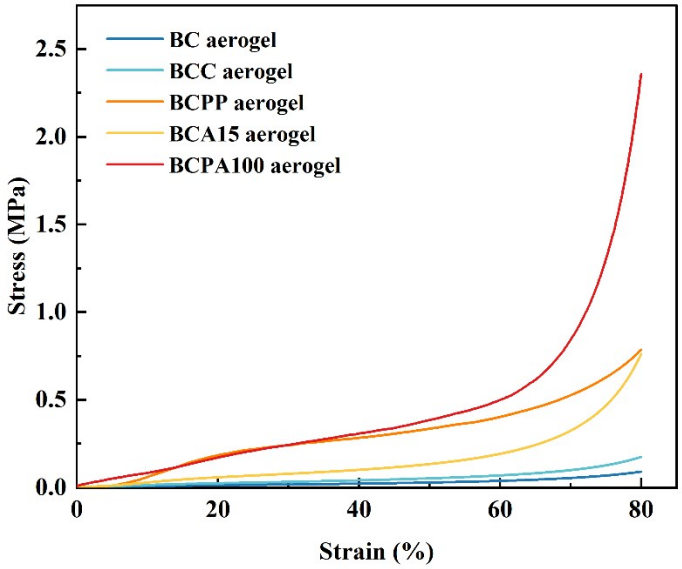

Fig. S11 Compressive stress-strain curve of BC aerogel (BC/GA), BCC aerogel (BC/GA/CMC), BCPP aerogel (BC/GA/PEI/PA), BCA15 aerogel (BC/GA/CMC/PEI) and BCPA100 aerogel (BC/GA/CMC/PEI/PA).

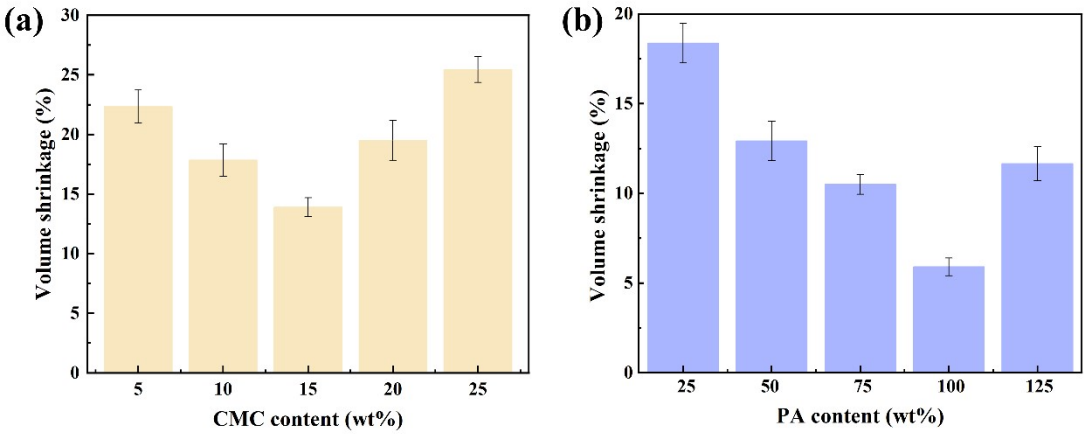

Fig. S12 The volume shrinkage ratio of BCA aerogels with different CMC content and BCPA aerogels with different PA content.

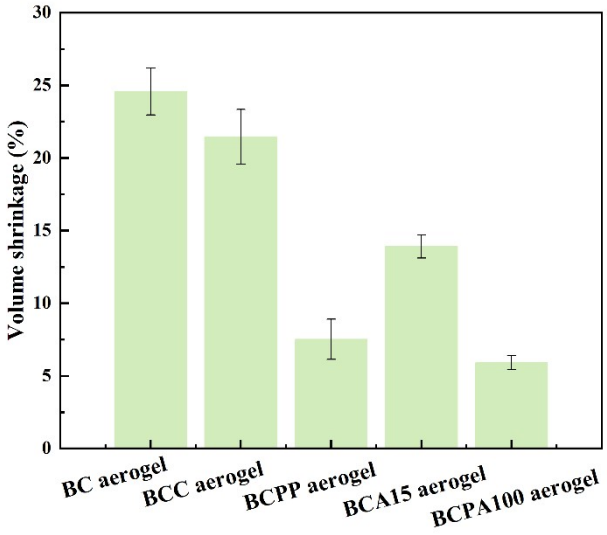

Fig. S13 Volume shrinkage of BC aerogel, BCC aerogel, BCPP aerogel, BCA15 aerogel and BCPA100 aerogel.

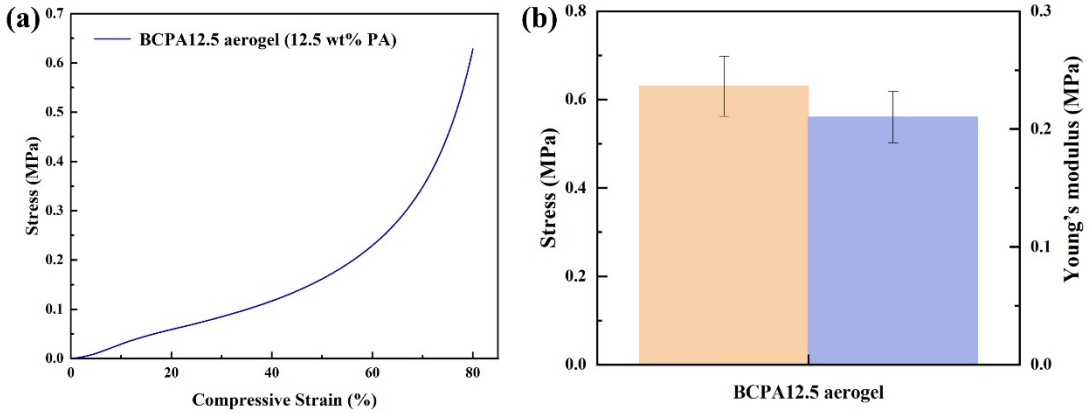

Fig. S14 Compressive stress-strain curve, compressive stress (ε=80%) and Young's modulus of BCPA12.5 aerogel.

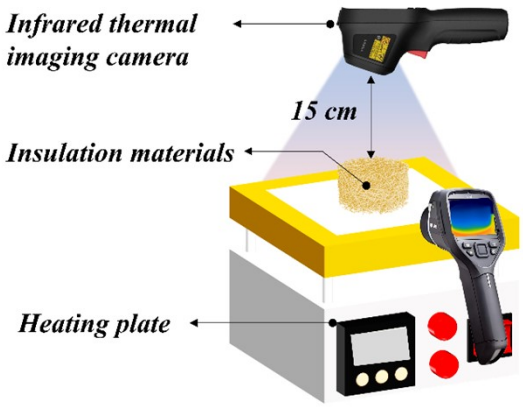

Fig. S15 Schematic illustration of the thermal insulation testing device when insulation materials were placed on a heating plate.

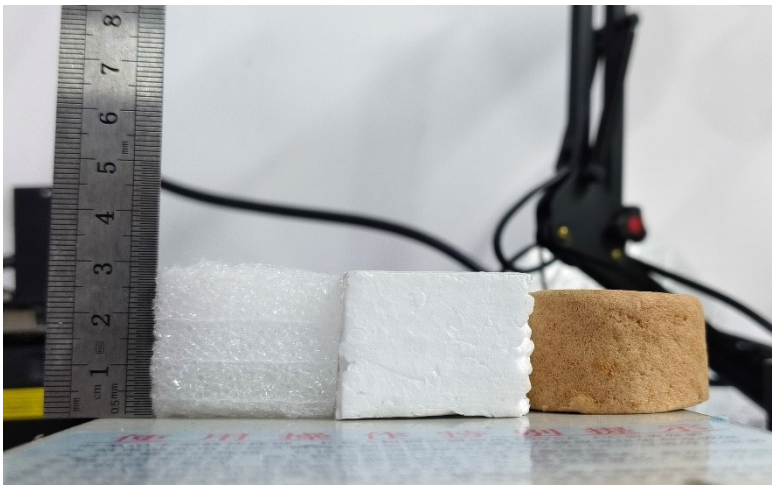

Fig. S16 Digital photos of EPE foam (left), EPE foam (middle) and BCPA100 aerogel (right) for thermal insulation test.

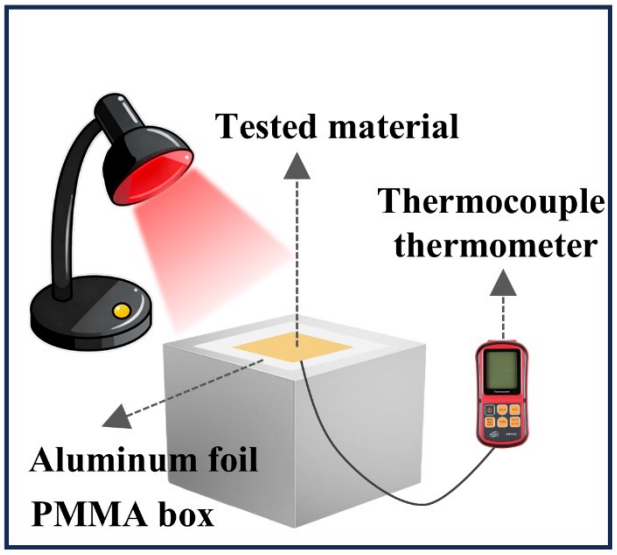

Fig. S17 Schematic illustration of the thermal insulation testing device for wood board and BCPA100 aerogel.

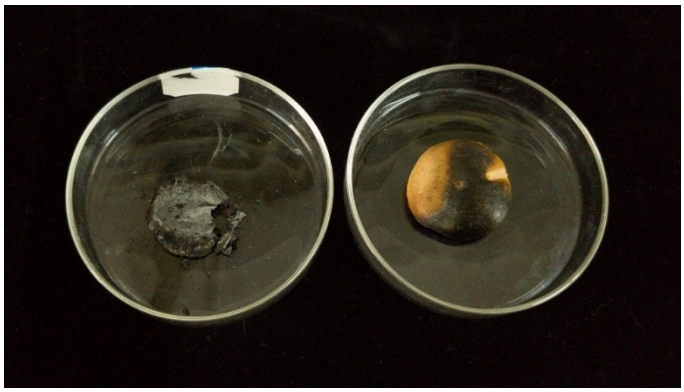

Fig. S18 Digital photos of BCA15 aerogel (left) and BCPA100 aerogel (right) after burning over an alcohol lamp.

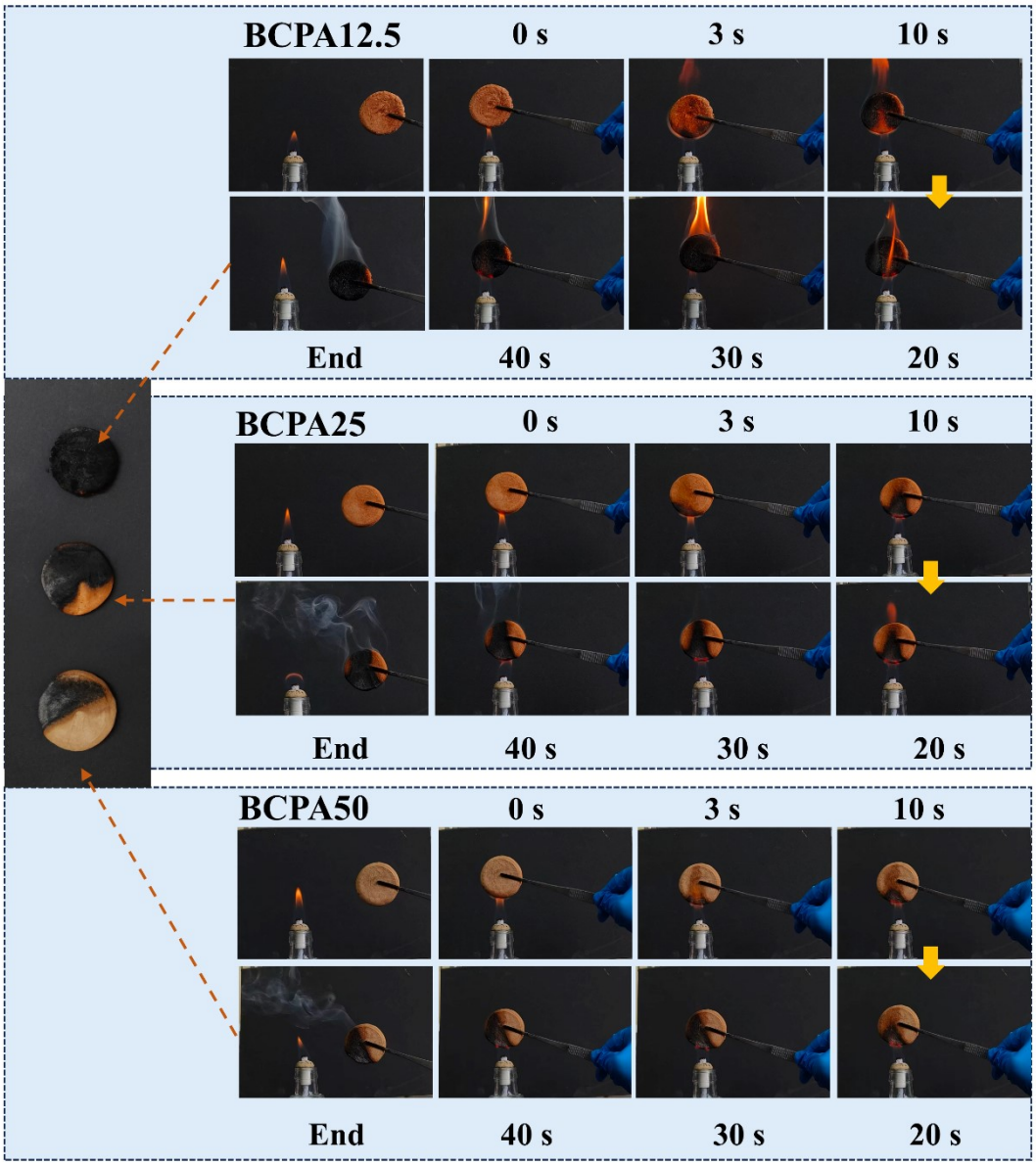

Fig. S19 Digital photos of BCPA12.5 aerogel, BCPA25 aerogel and BCPA50 aerogel upon exposure to the flame of an alcohol lamp.

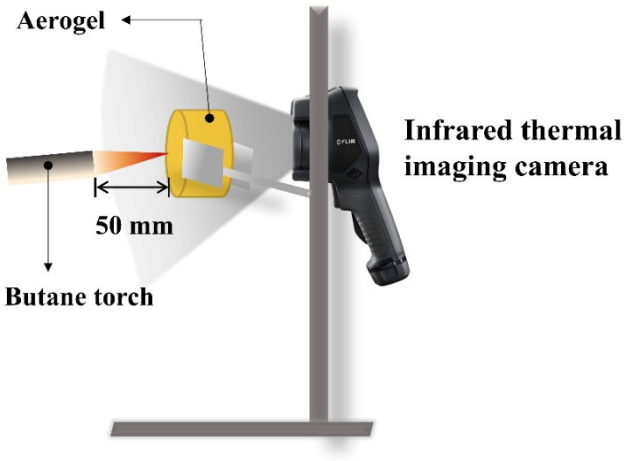

Fig. S20 Schematic illustration of the flame retardancy testing device for BCPA aerogels fired using by a butane torch (~1300 ℃).

Fig. S21 Digital photos of BCPA100 aerogel before and after butane torch flame test.

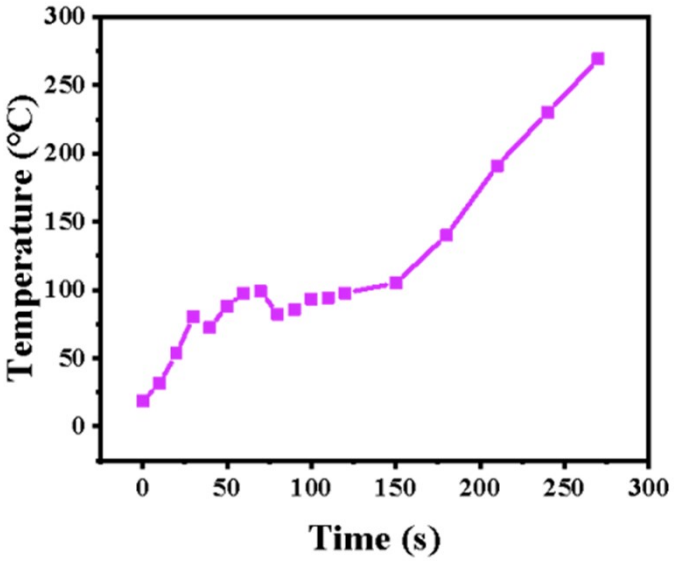

Fig. S22 Surface temperature variation of BCPA100 aerogel over time during butane torch exposure.

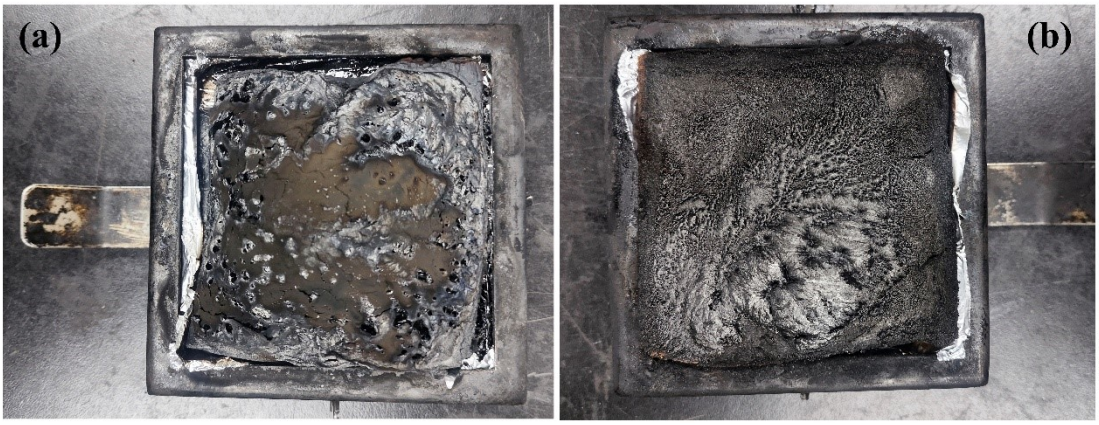

Fig. S23 Photographs of (a) BCA15 aerogel and (b) BCPA100 aerogel after cone calorimetry test.

Table S1. Preparation conditions of BCA aerogels and BCPA aerogels.

Code	Cellulose content (wt%)	PEI content (wt%, based on cellulose suspension)	GA content (wt%, based on cellulose suspension)	CMC content (wt%, based on cellulose mass)	Effective PA content (wt%, based on cellulose mass)
BCA5	3	2	2	5	0
BCA10				10	0
BCA15				15	0
BCA20				20	0
BCA25				25	0
BCPA25	3	2	2	15	25
BCPA50				15	50
BCPA75				15	75
BCPA100				15	100

BCPA125			15	125

Table S2. Preparation conditions of control aerogel samples.

Code	Cellulose content (wt%)	PEI content (wt%, based on cellulose suspension)	GA content (wt%, based on cellulose suspension)	CMC content (wt%, based on cellulose mass)	Effective PA content (wt%, based on cellulose mass)
BC	03	0	2	0	0
BCC		0	2	15	0
BCPP		2	2	0	100

Table S3. The key thermal degradation temperatures, maximum decomposition rates and residual weights of BC-GA/CMC aerogel, BCA15 aerogel and BCPA100 aerogel under an oxygen atmosphere.

Samples	Tonset (℃)	Tmax (℃)	(dW/dt)max (%/min)	Residual weight (%)
BC-GA/CMC aerogel	278.0	314.7	-10.95	8.46
BCA15 aerogel	301.1	314.9	-9.13	2.95
BCPA100 aerogel	272.0	283.3	-7.29	19.19

Table S4. Preparation and performances comparison of recent reported cellulose aerogels and foams.

Aerogels/Foams	Preparation method	Volume shrinkage (%)	Porosity (%)	Density (g/cm^3)	Thermal conductivity ($W \cdot K^{-1} \cdot m^{-1}$)	Compressive Strength (MPa)	Ref
Date palm-derived cellulose aerogels	Cellulose dissolution; freeze-drying	NA	94.16-96.31	0.055-0.085	0.038-0.074	0.5 (50%)	[1]
Cellulose/clay composite aerogel	Vacuum filtration; freeze-drying	NA	NA	0.14	0.047	2.638 (80%)	[2]
Bamboo fiber/microfibrillated cellulose foam	Mechanical stirring foaming; ambient drying	27.67	NA	0.05-0.12	NA	0.0227 (60%)	[3]
Lignocellulose foam	LiOH/urea/H_2O dissolution system; freeze-drying	NA	94.93	0.062	0.046	0.2-1.2 (70%)	[4]
Cellulose/bentonite foam	NaOH/urea dissolution system; ambient drying	8-16	90.92	0.09	0.063	3.4 (40%)	[5]
BCA15 aerogel	Schiff base reaction; ambient drying	13.90	95.99	0.0578	0.0351	0.81 (80%)	**This work**
BCPA100 aerogel	Schiff base reaction; ambient drying	5.90	94.51	0.0818	0.0333	2.31 (80%)	**This work**

References

[1] H. Al Abdallah, J. H. Tannous and B. Abu-Jdayil, *Dev. Built Environ.*, 2025, **24**, 100773.

[2] M. Wang, H. Cao, Z. Huang, Z. Lin, S. Ye, Y. Li, Y. Hua, Z. Wei and Y. Zhao, *Compos. Part B Eng.*, 2026, **309**, 113098.

[3] Y. Feng, Y. Yu, T. Xi, L. Chen, X. Wang, T. Xu, H. Xiao, Z. Wang, H. Dai and H. Bian, *Adv. Funct. Mater.*, 2025, **36**, e14273.

[4] H. Dong, S. Wei, W. Chen, B. Lu, Z. Cai, B. Yang, X. Li and X. Li, *ACS Nano*, 2025, **19**, 11712–11727.

[5] L. Chen, S. Wang, S. Wang, C. Chen, L. Qi, L. Yu, Z. Lu, J. Huang, J. Chen, Z. Wang, X. Shi, Z. Song, H. Liu and C. Chen, *ACS Nan*o, 2022, **16**, 16414–16425.